

 Very Important Paper

 Special Collection

# Electrocatalysis Beyond 2020: How to Tune the Preexponential Frequency Factor

 Praveen Narangoda,<sup>[a]</sup> Ioannis Spanos,<sup>[a]</sup> Justus Masa,<sup>[a]</sup> Robert Schlögl,<sup>[a, b]</sup> and Aleksandar R. Zeradjanin<sup>\*[a]</sup>

After a century of research on electrocatalytic reactions, a universal theory of electrocatalysis is still not established due to limited understanding of complex energy conversion processes at electrified electrode-electrolyte interfaces. Most of the research efforts directed toward the acceleration of important electrocatalytic reactions (e.g. hydrogen evolution reaction) were in the direction of minimizing activation energy by tuning the adsorption energies of key intermediates. This kind of approach is well-established and, importantly, in some cases it was valuable by predicting the design of electrocatalysts with

advanced properties. However, in some very important research endeavors, advancement in performance of newly designed electrocatalysts could not be attributed to altered/minimized activation energy. Important to note is that modern electrocatalysis almost completely disregards influence of the preexponential factor on reaction rate. In this work, we open some important questions relevant for future of electrocatalysis and electrochemical energy conversion, with special focus on preexponential factor as major contributor to electrocatalytic reaction rate.

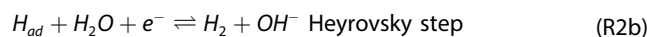
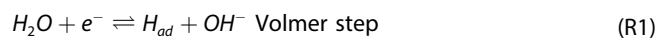
## Introduction

This research article is written on the occasion of the 65<sup>th</sup> birthday of Prof. Wolfgang Schuhmann, a veteran of electrochemistry and one of the last electrochemists who dealt with almost every field of electrochemistry (photoelectrochemistry, bioelectrochemistry, sensors, electroanalysis, corrosion, electrocatalysis etc.). During his very successful academic career as a researcher, teacher, organizer and mentor, he contributed in various ways to the development of science. Certainly, one of the most important contributions he made is that he did not hesitate to encourage determined young scientists in their research endeavors, no matter how unconventional their ideas may appear to be. Being open minded and supportive towards young researchers who are pushing existing frontiers of scientific knowledge and creating their own research identity and environment; is what we could recognize as one of the most important contributions of Prof. Schuhmann's legacy in electrochemical research.

Approximately ten years ago, Schuhmann's group published a paper in ChemSusChem entitled: "Role of Water in the

Chlorine Evolution Reaction at RuO<sub>2</sub>-Based Electrodes-Understanding Electrocatalysis as a Resonance Phenomenon".<sup>[1]</sup> That was one of the pioneering works that implicitly suggested that structural dynamics formally observed through Arrhenius' preexponential frequency factor could have a much larger role in electrocatalysis than anticipated by the conventional view which suggests predominant importance of activation energy. Continuing on that track, this work analyzed the impact of the preexponential frequency factor on the kinetics of the hydrogen evolution reaction (HER) in alkaline media, as well the manifestation of interplay between the preexponential frequency factor and activation energy for the case of the HER in alkaline media.


In alkaline electrolytes, the HER proceeds via the following elementary steps (Reactions 1 and 2):





Adsorbed intermediate species (H<sub>ad</sub>) formation in Volmer's step (React.1) by cathodic reduction of water molecule is coupled with the release of a hydroxyl-ion into the electrolyte. Molecular hydrogen will be formed by recombination of two H<sub>ad</sub> from two neighboring active sites in Tafel's step (React.2a) or by interaction of H<sub>ad</sub> with an electron and a water molecule followed by release of a hydroxyl-ion in Heyrovsky's step (React.2b). The specificity of the HER in alkaline media is that water is a reactant and direct source of the intermediates. Importantly, interfacial water molecules could have an indirect role behaving as promoters or inhibitors for HER.<sup>[2,3]</sup> In the past only few research groups insisted on very special role of interfacial water in the HER mechanism, where theoretical works

[a] Dr. P. Narangoda, Dr. I. Spanos, Dr. J. Masa, Prof. Dr. R. Schlögl, Dr. A. R. Zeradjanin  
 Max Planck Institute for Chemical Energy Conversion  
 Stiftstrasse 34–36, 45470 Mülheim an der Ruhr, Germany  
 E-mail: aleksandar.zeradjanin@cec.mpg.de

[b] Prof. Dr. R. Schlögl  
 Fritz-Haber-Institut der Max-Planck Gesellschaft  
 Faradayweg 4–6, 14195 Berlin, Germany

 Supporting information for this article is available on the WWW under <https://doi.org/10.1002/celec.202101278>

 An invited contribution to the Wolfgang Schuhmann Festschrift

 © 2021 The Authors. ChemElectroChem published by Wiley-VCH GmbH. This is an open access article under the terms of the Creative Commons Attribution License, which permits use, distribution and reproduction in any medium, provided the original work is properly cited.

of Schmickler et al.<sup>[4]</sup> and experimental works of Markovic et al.<sup>[2]</sup> definitely deserve attention. Up to now despite lack of experimental studies that should give satisfactory dynamic picture about interfacial water structure during HER, computational chemists have made substantial progress in describing of electrified solid/liquid interfaces including: 1) assessment of solvent effects on adsorption energies with relatively accurate determination of onset potential,<sup>[5]</sup> 2) pH effects on interfacial water structure and reaction kinetics,<sup>[6,7]</sup> 3) analysis of competition between water–metal and water–water interaction as the structure-determining factors whether water at metal surfaces is ice-like or not<sup>[8]</sup> including changes in the work function of the metal while interacting with interfacial water dipoles.<sup>[9]</sup> Taking into consideration that during HER the electrode surface is negatively charged, some authors assumed that water molecules will be physisorbed/adsorbed at the electrode surface through hydrogen atom(s),<sup>[10,11]</sup> however for metal–water interaction, it is most probably via one of the two nonbonding electron pairs of the oxygen atom.<sup>[12]</sup> In our understanding, electrostatic interaction between d-orbitals of a metal and the nonbonding electron pair of the oxygen atom at cathodic potentials is not favored and it can only proceed at very oxophilic metallic surfaces. Oxophilic surfaces could deprotonate water easily and supply protons that are subsequently reduced to form H<sub>ad</sub>. However, besides H<sub>ad</sub> at the surface, decoupled HO<sub>ad</sub> should also be reduced and then desorbed from the surface. Therefore, the mechanism of H<sub>ad</sub> formation from alkaline media is complex because it is coupled with HO<sub>ad</sub> formation that does not participate in hydrogen molecule generation, nevertheless it has to be removed from the surface to make active sites accessible for HER. On this basis, it is

intuitive to assume that cathodic water discharge should be more energetically demanding than the reduction of proton from acidic electrolytes. A schematic illustration of hydrogen adsorption in alkaline electrolytes is given in Figure 1.

Evidently, the kinetics of HER in alkaline media depends on the adsorption energy of H<sub>ad</sub> formation, as well as on the desorption energy for OH<sub>ad</sub> removal. This kind of mechanism was discussed by Markovic et al.<sup>[13,14]</sup> however, they did not explicitly postulate that cathodic water discharge (React.1a) is actually the sum of one anodic reaction (electrochemical water deprotonation, Figure 1b) and two cathodic reactions (proton reduction and HO<sub>ad</sub> reduction, Figure 1b and Figure 1d).

The conventional view on electrocatalysis, based on the Sabatier principle, suggests that exchange current density is predominantly influenced by the adsorption energies of the key intermediates.<sup>[15–19]</sup> In other words, an electrocatalyst will have a high exchange current if intermediates are neither too strongly nor too weakly bonded on the electrode surface. However, there are also other parameters influencing exchange current density.<sup>[4,20–25]</sup> In more quantitative terms, the exchange current (*j*<sub>0</sub>) is illustrated with Eq. 1

$$j_0 = nF c^p(\text{OH}^-) c^q(\text{H}_2) (1 - \theta) k_{et} \exp\left(\frac{-\beta F E_{rev}}{RT}\right) \exp\left(\frac{-\gamma \Delta G_{ad}}{RT}\right) \quad (1)$$

Where: *n* – number of exchanged electrons, *F* – Faraday's constant, *c*(OH<sup>−</sup>) – concentration of hydroxyl ions, *c*(H<sub>2</sub>) – concentration of dissolved hydrogen, *p* – partial order with respect to hydroxyl ion concentration, *q* – partial order with

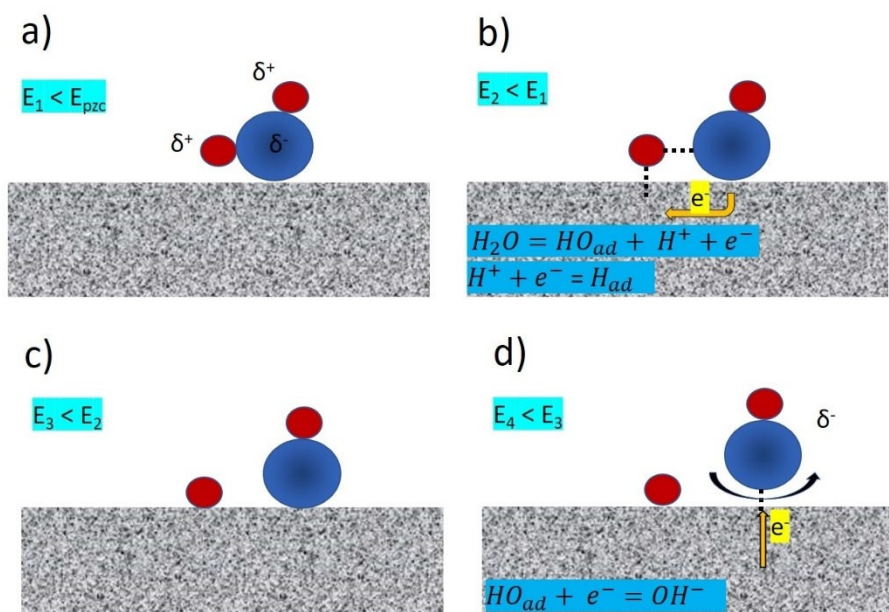


**Figure 1.** Formation of H<sub>ad</sub> intermediate from water molecule in alkaline electrolyte under cathodic polarization. The scheme illustrates the processes in the first elementary step of the HER (React.1) where: a) single water molecule at electrode surface at potential (*E*<sub>1</sub>) more negative than potential of zero charge (*E*<sub>pzc</sub>), bonded on the surface through oxygen (blue) atom and having at least one of the hydrogen atoms (red) in close proximity to the surface; b) with further polarization (*E*<sub>2</sub> < *E*<sub>1</sub>) hydrogen atom that was closer to the negatively charged surface is getting attracted by the electrode, simultaneously weakening the bond with oxygen, causing water deprotonation c) formation of H<sub>ad</sub> and HO<sub>ad</sub>; d) “cleaning” of the surface by HO<sub>ad</sub> reduction.

respect to dissolved hydrogen concentration,  $\theta$  – total coverage including intermediate ( $H_{ad}$ ) and  $HO_{ads}$ ,  $k_{et}$  – electron transfer rate constant,  $\beta$  – symmetry factor,  $E_{rev}$  – reversible potential,  $R$  – universal gas constant,  $T$  – temperature,  $\Delta G_{ad}$  – adsorption energy of intermediate formation,  $\gamma$  – Bronsted-Evans-Polanyi coefficient. It is important to notice that water deprotonation is prerequisite for proton reduction (Figure 1b), so the adsorption energy for intermediate formation is the sum of the adsorption energies for  $H_{ad}$  as well as  $HO_{ad}$  formation. Consequently, from Eq. 1 it can be concluded that exchange current is controlled via adsorption energies by a delicate balance between activation energy (through  $\Delta G_{ad}$ ) and preexponential factor (through  $(1-\theta)$ ), resulting in a “volcano”-type dependence between  $\log j_0$ - $\Delta G_{ad}$ . However, other parameters that determine activation energy (symmetry factor and Bronsted-Evans-Polanyi coefficient) as well as parameters that influence the preexponential factor (partial order with respect to hydroxyl ion concentration, partial order with respect to dissolved hydrogen concentration and electron transfer rate constant) also depend on the nature of electrode material and they can distort the balance between activation energy and preexponential factor that is expected from Sabatier principle.

## Results and Discussion

### HER Activity Trends in Alkaline Media

In Figure 2 are activity trends for HER on 15 metals in 0.1 M KOH recorded at temperatures of 20 °C and 50 °C, expressed as overpotential at a current density of 10 mA cm<sup>-2</sup>. Most of the metals are from the d-block with the exception of two sp-metals that are analyzed in addition, to get insight into the difference between HER in the d-block metals and the sp-metals.

The most active HER catalysts in alkaline media are noble metals, as suggested in the literature, with Ir being the most active, as also reported by Markovic et al.<sup>[26]</sup> The activity trend at temperature of 20 °C for the analyzed metals was in the order:

Ir > Rh ≈ Ru ≈ Re > Pt > Ni > Co ≈ Fe > Mo > Pd > Ag > Cu > Au > Bi > Pb, where after Ir the most active were Rh, Ru, Re, Pt and Ni with very similar performance, followed by almost identical activity of Fe and Co, followed by very similar performance by Mo and Pd. All these metals are in the span of overpotential between 0.25 V up to 0.47 V. The coinage metals (Ag, Cu and Au) had substantially larger overpotentials spanning from 0.64 V up to 0.86 V and finally sp metals (Bi and Pb) that exhibited the highest overpotentials spanning in the range from 1.18 V up to 1.45 V. At 50 °C, the HER activity trend looks a bit different in comparison to that at 20 °C: Ir > Pt > Rh > Ru > Pd > Re > Ni > Fe > Mo > Co > Cu > Ag > Au > Bi > Pb. The general pattern that could be recognized at both temperatures is that after the noble metals, that are the most active HER electrocatalysts, the second most active group are the triad of iron, then the coinage metals and at the end the sp-metals, with unusual, almost inverse, temperature dependence of Co, Ag and Au. This could be due to anomalous temperature dependence of the Tafel slope (drop of Tafel's slope with temperature)<sup>[27–30]</sup> or due to phenomena of negative activation energy<sup>[31]</sup> also known as anti-Arrhenius behavior.<sup>[32]</sup> Both phenomena are beyond the scope of this particular analysis, but they will be analyzed in future works.

### “Dissection” of the Rate Law

The activity trends given above are in the form of overpotential, that is a complex kinetic quantity given by Eq. 2:

$$\eta = b \log \frac{j}{j_0} \quad (2)$$

Where  $\eta$  – overpotential at a defined current density,  $j$  – current density,  $j_0$  – exchange current and  $b$  – Tafel's slope. From Eq. 2, it is straightforward that overpotential at fixed current density will be reduced if the exchange current is higher and/or Tafel's slope is lower. Whereas exchange current (Eq. 1.) corresponds to reaction rate at equilibrium potential, Tafel's

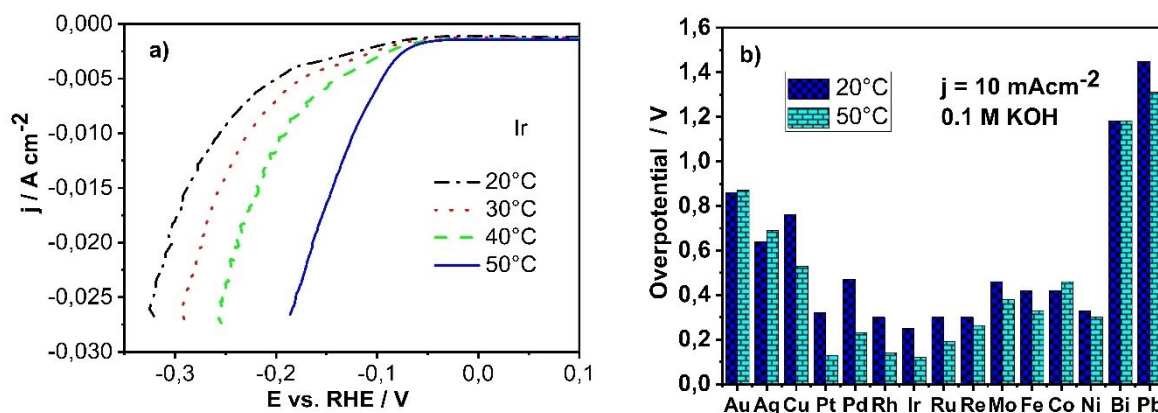


**Figure 2.** a) Example of temperature dependent HER polarization curves recorded in 0.1 M KOH on polycrystalline Ir electrode using linear sweep voltammetry (LSV) with sweep rate of 5 mVs<sup>-1</sup>. b) HER activity trend for 15 metals in 0.1 M KOH at temperatures of 20 °C and 50 °C given as overpotential at a current density of 10 mA cm<sup>-2</sup>.

slope is a kinetic parameter that depends on the symmetry factor that is a parameter linked to the shape of the activation barrier and depicts how flexibly one can alter the activation barrier with electrode potential. It remains unclear for decades how exactly to tune the symmetry factor and what material and/or interfacial property controls value of the symmetry factor. Nevertheless, present widely held assumption that the symmetry factor always has a value of 0.5 has no real foundation, which nowadays can be supported by computational models.<sup>[33–35]</sup> Therefore, the intrinsic link between exchange current and Tafel's slope is unknown. Therefore, if one intends to establish any relevant structure-activity relations, all parameters that are comprised in the exchange current (Eq. 1.) as well as all parameters in the Tafel slope expression<sup>[36]</sup> have to be analyzed as a function of relevant material or interfacial descriptors (e.g. number of outer electrons).<sup>[37,38]</sup> A schematic illustration of the rate law dissection is given in Figure 3. Most of the properties are defined in Eq. 1. except:  $E_{\text{act}}$  – activation energy;  $A$  – preexponential factor,<sup>[39,40]</sup>  $E_{\text{M-H}}$  – intermediate bond strength energy, that is linked with intermediate adsorption energy;  $E_{\text{M-H}_2\text{O}}$  – energy consumed for metal–water interaction or water bilayer reconstruction during HER,<sup>[41]</sup>  $A_{\text{lat.vib}}$  – hypothetical contribution of individual and collective lattice vibrations to effective collisions;  $A_{\text{tun}}$  – hypothetical contribution of proton tunneling to product formation. In order to summarize briefly the scheme given in Figure 3, we could note the following: 1) overpotential at defined current density is determined by exchange current (close to equilibrium kinetic parameter) and Tafel's slope (far from equilibrium kinetic parameter). 2) exchange current can be further split into activation energy that depends on the magnitude of the activation barrier of the rate determining step and the preexponential factor that defines overall number of effective collisions of reactant with electrode surface which result in product formation 3) activation energy depends on the intermediate adsorption energy, energy required to reconstruct

the water bilayer at the electrode surface during HER and from the shape of the activation barrier that can be altered by adsorption and/or electrode potential<sup>[22]</sup> 4) preexponential factor depends on partial orders with respect to reactants which define how concentration of the reactants/products contribute to effective collisions, on the available/accessible fraction of active sites,<sup>[42]</sup> further (hypothetically) on individual and collective lattice vibrations that potentially influence the frequency of effective collisions<sup>[23]</sup> as well as on proton tunneling.<sup>[43–45]</sup>

### Phenomenological Relation between Exchange Current and Tafel Slope

The first step in dissection of the rate law would be to observe the exchange current vs. Tafel's slope relation. The possible phenomenological relation between exchange current and Tafel's slope for HER in alkaline media, to the best of our knowledge, was never reported. This relation could highlight whether close-to-equilibrium HER activity trends overlap with far from equilibrium activity trends, particularly, far-from-equilibrium trends that correspond to current densities of tens of  $\text{mA cm}^{-2}$ . From Figure 4, we could analyze the actual interrelationship between the exchange current and Tafel's slope for HER in alkaline media.

From Figure 4, one can notice that for series of the d-metals, values of the exchange currents span over six orders of magnitude. Tafel's slopes have values from approximately 100 mV/dec up to approximately 300 mV/dec. In the literature were discussed some controversies considering exact values of kinetic parameters obtained on different experimental setups,<sup>[46,47]</sup> however, as shown previously, accurate values of kinetic parameters are challenging to obtain at gas evolving electrodes even on well-defined systems like rotating disc electrodes (RDE).<sup>[48]</sup> This is due to gas-bubble adherence on electrode surfaces that results in unknown coverage of active

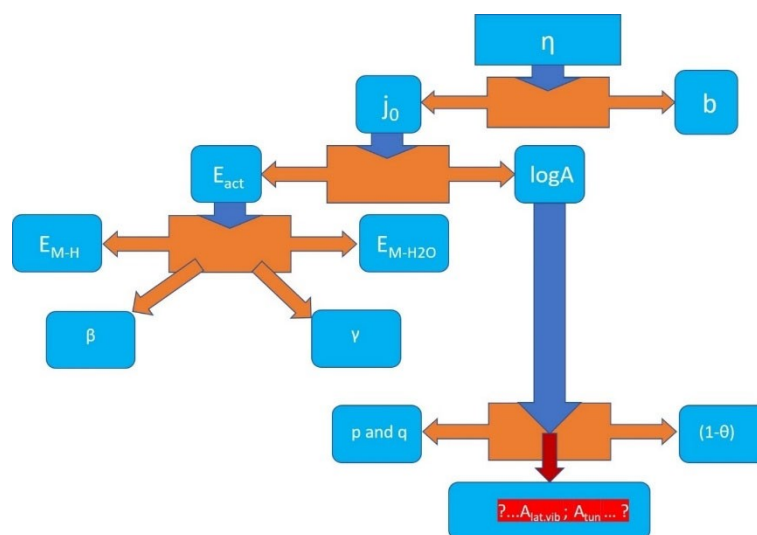


**Figure 3.** Schematic representation of the rate law “dissection” with indication of the relevant parameters that could be potentially linked with material properties or interfacial properties of the electrode/electrolyte boundary.

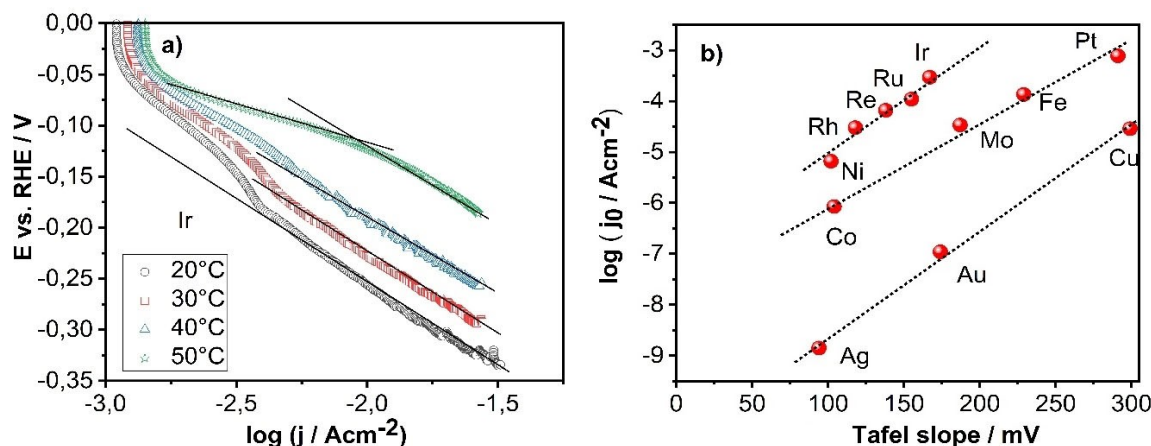


**Figure 4.** a) Example of Tafel plots for HER on Ir at various temperatures used for extraction of Tafel slope and exchange current density in 0.1 M KOH. b) Interrelation between exchange current and Tafel slope for HER on 12 d-metals in 0.1 M KOH.

sites,<sup>[49]</sup> which in turn makes the effective surface area unknown and somewhere between geometric area and the total area at open circuit conditions.<sup>[48,50]</sup> Also, one should not undermine the influence of impurities on measurements.<sup>[51–53]</sup> Therefore, it is more relevant to analyze trends. The general tendency is that increase in exchange current is linked with increase in Tafel's slope. This interrelation reveals that electrode kinetics for HER in alkaline media suffer from intrinsic limitations manifested through a delicate balance between reaction rate at equilibrium and the shape of the activation barrier far from equilibrium. In other words, metals that have high reaction rate close to equilibrium, exhibit, a shape of the activation barrier that is difficult to overcome with electrode potential far from equilibrium. In Figure 4 one can notice that metals are distributed in three groups: 1) coinage metals that exhibit the lowest exchange currents 2) iron triad and early transition metals that have intermediate values of exchange currents and 3) noble metals that exhibit the highest values of exchange currents. Surprising from the overall pattern, are the positions of Ni and Pt. Ni should in principle follow the pattern of the iron triad, while Pt should follow the pattern of the noble metals. However, it seems that activity trends comprise a complexity that is still beyond comprehension. While the exchange currents noticeably have values comparable to the values shown in the literature for acidic media,<sup>[17]</sup> Tafel's slopes are much higher than in acidic media. One of the reasons for generally high Tafel's slopes can be the energetically demanding cathodic water discharge, as discussed above. If we recall scheme shown in Figure 1, water discharge comprises of three processes: 1) water deprotonation and electron transfer towards the Fermi level of the metal 2) proton reduction and 3) HO<sub>ad</sub> reduction and desorption. Each of these processes, besides adsorption/desorption, is coupled with electron transfer. To have these three processes simultaneously at the same electrode potential is not probable, so at least one of the three processes will be energetically very demanding, which could be reason for high value of Tafel's slope. Interfacial water molecules/layers have a special role during electrocatalysis but

their exact function is still largely unknown.<sup>[2]</sup> Analysis of Trasatti suggests that metals that are strongly binding hydrogen from the gas-phase will weakly bind hydrogen in an electrochemical environment.<sup>[54]</sup> Besides influencing bond strength, interfacial water dipoles have a special role in the complex interface dynamics.<sup>[3,24]</sup> Koper et al. proposed that in alkaline media the interfacial water network, at the potential of HER, interacts strongly with the strong interfacial electric field and is therefore more rigid and more difficult to reorganize during the charge transfer through the electrical double layer.<sup>[3]</sup> Strength of electric field is determined by the distance of the Epzc from the reversible potential for HER or from working electrode potential. However, as shown previously by Trasatti, metals that have the largest difference between Epzc and reversible potential are actually the most active for HER in acidic media.<sup>[12,17]</sup> This is due to the fact that metals with very positive Epzc (e.g. Pt) are strongly negatively charged at reversible potential for HER, which causes the double layer to be filled with protons whose solvation spheres are destabilized.<sup>[21,22,24]</sup> So the behavior of metals during HER in acidic media is clearly in disagreement with conclusions of Koper et al.<sup>[3]</sup> Although Koper's notion cannot explain the well-established experimental correlation of Trasatti between the E<sub>pzc</sub> and the exchange current density in acidic media, it is not necessarily wrong. It might be possible that an optimal surface charge at the electrocatalytic electrode, which establishes a delicate balance between the activation entropy and the activation enthalpy, is responsible for overall activity, as hinted by Schmickler et al.<sup>[55]</sup> Therefore of utmost importance is to analyze interrelation between activation energy and preexponential factor to comprehend from where exactly enhancement in electrocatalytic activity originates from.

### Activation Energy vs. Preexponential Frequency Factor

From temperature dependence of exchange current (example given for Ir in Figure 5a) one can obtain activation energy for HER as well as preexponential frequency factor for HER on the

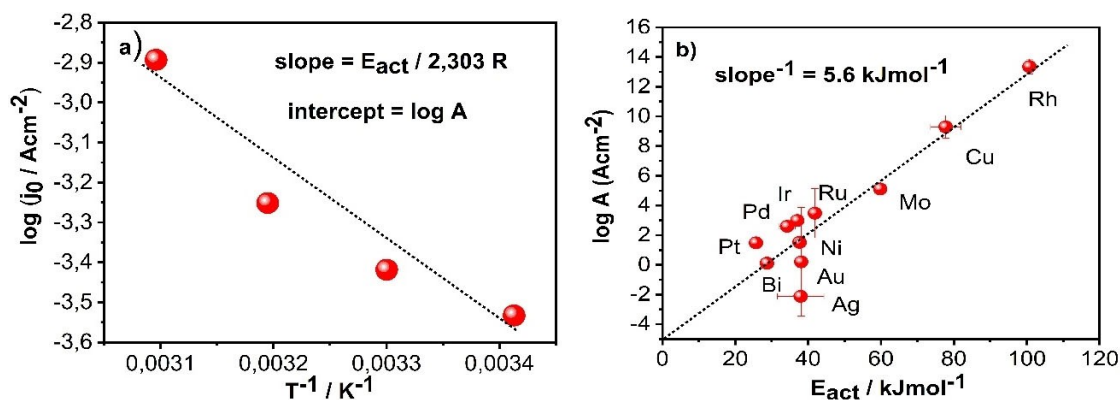


**Figure 5.** a) Example of Arrhenius plot for electrocatalytic HER on Ir in 0.1 M KOH. b) Relation between activation energy and preexponential frequency factor for HER in 0.1 M KOH.

analyzed metals in 0.1 M KOH. Due to the fact that Fe, Co, Re and Pb exhibit the so called negative activation energy<sup>[31]</sup> (in electrocatalysis manifested as a drop in exchange current with temperature increase), they are excluded from further discussion. In Figure 5b is given a correlation between activation energy and preexponential frequency factor for HER in 0.1 M KOH. The correlation is linear and suggests that if the activation energy is reduced by  $5.6 \text{ kJ mol}^{-1}$ , the preexponential frequency factor will decrease by an order of magnitude. The underlying reasons for this kind of balance have not yet been fully elucidated in electrocatalysis. Similar phenomena, called compensation effect, is well known in thermal catalysis.<sup>[56–60]</sup> In the modern era of thermal catalysis, it is accepted that the intrinsic reason for the compensation effect is interplay between adsorption energy in the exponential factor and the  $(1-\theta)$  term in the preexponential factor, which is formally perceived as interplay between activation enthalpy and activation entropy.<sup>[56]</sup> This explanation cannot apply in electrocatalysis.

Activation energies are in the range from approximately  $25 \text{ kJ mol}^{-1}$  for Pt up to approximately  $100 \text{ kJ mol}^{-1}$  for Rh. Preexponential frequency factors ranged from approximately  $\log A \approx -2$  for Ag up to approximately  $\log A \approx 14$  for Rh, spanning almost 16 orders of magnitude for the different metals. Interestingly, activation energies for Pt and Rh are drastically different despite the fact that they exhibit similar overpotential. This example reveals that reduction of activation energy by tuning adsorption energies of intermediates is not a universal way to enhance electrocatalytic activity. The large differences observed in the preexponential frequency factor amongst different metals cannot be exclusively ascribed to the  $(1-\theta)$  term, which suggests that comprehensive treatment of electrocatalysis has to advance beyond the paradigm of adsorption energies. We need a more comprehensive view on the dynamic aspects of the activation process for a deeper understanding of the key contributors to the preexponential frequency factor.

## Conclusions

On the example of HER in alkaline media, it was shown that future research endeavors in the field of electrocatalysis will require in-depth analysis of the preexponential frequency factor, its relation to activation energy and its impact on electrocatalytic reaction rate. The observations made from dissection of the rate law lead us to propose that all variables that contribute to reaction rate (minimum 8 of them) should be separately analyzed as a function of relevant material properties or interfacial properties to underpin the origins of activity for a particular electrocatalyst. Only this kind of approach will allow in-depth comprehension of the origins of electrocatalytic activity, discovery of new relevant descriptors as well as further design and fine-tuning of new advanced electrocatalysts. From this phenomenological approach, we can conclude at this point, that exchange current and Tafel' slope are directly proportional, meaning that for electrocatalysts that exhibit high reaction rates close to equilibrium, it is difficult to alter the activation barrier far-from-equilibrium with electrode potential. At the same time, activation energy and preexponential frequency factor are also directly proportional with a linear dependence that suggests that if one reduces the activation energy by  $5.6 \text{ kJ mol}^{-1}$ , the preexponential factor will drop by an order of magnitude. This suggests that reduction of activation energy is not necessarily successful way to enhance electrocatalytic activity. A future priority is to conduct very careful studies on the interrelation between preexponential factor and activation energy to decipher the intrinsic link between these two parameters.

## Experimental Section

Electrochemical measurements were conducted in a home-made temperature controlled electrochemical cell constructed out of PEEK (Polyether ether ketone). Working electrodes were 16 polycrystalline metals (MaTeck, Juelich, Germany) with a thickness of 3 mm and diameter of 5 mm, polished using SiC papers (400, 800, 1200 and 2400 grit) and alumina paste ( $1.0\text{--}0.05 \mu\text{m}$ ), washed with 1 M KOH, followed by de-ionized water and immediately dried

under a stream of argon and finally inserted into a Teflon holder as RDE (rotating disc electrode) tip controlled by a rotator (Autolab, Methrom, Switzerland) at 1600 rotations per minute. The potential of the working electrode was controlled using a potentiostat/galvanostat (Biologic, VSP with EIS, France). Counter electrode was graphite rod and reference electrode was commercial Hg/HgO with saturated 0.1 M KOH (CH Instruments, Texas, USA...). Temperature was controlled with a thermostat (Huber CC-K6, Germany) in the range 293–323 K. Temperature drift of reference electrode vs. RHE 1.125 mV/°C. Electrolyte was 0.1 M KOH made by dilution out of 1 M KOH (Fluka™ KOH concentrate solution for 1 L, 1 M KOH volumetric solution, Honeywell Chemicals, Germany) and ultrapure deionized water (ELGA, PURELAB flex system with a resistivity of 18.2 MΩ cm, Celle, Germany). Polarization curves were recorded in the potential range from 0.1 V vs. RHE up to a potential where a current density of 25 mA cm<sup>-2</sup> was reached with a scan rate of 5 mV/s. Ohmic drop correction was conducted using electrolyte resistance, respectively, extracted by impedance spectroscopy at open circuit conditions and under applied overpotentials. Additionally, impedance data were collected using the Mott-Schottky operational mode where capacitance is measured as a function of the applied potential. The employed AC (alternate current) perturbation was 10 mV using frequencies between 1 and 100 000 Hz. The electrical equivalent circuit (EEC) for the potential region of interest is constructed from an analytical model. Details were given previously.<sup>[61]</sup>

## Acknowledgements

Open Access funding enabled and organized by Projekt DEAL.

## Conflict of Interest

The authors declare no conflict of interest.

**Keywords:** electrocatalysis · water splitting · hydrogen evolution · alkaline electrolyte · preexponential factor

- [1] A. R. Zeradjanin, N. Menzel, P. Strasser, W. Schuhmann, *ChemSusChem* **2012**, *5*, 1897–1904.
- [2] J. Staszak-Jirkovský, R. Subbaraman, D. Strmcnik, K. L. Harrison, C. E. Diesendruck, R. Assary, O. Frank, L. Kober, G. K. H. Wiberg, B. Genorio, J. G. Connell, P. P. Lopes, V. R. Stamenkovic, L. Curtiss, J. S. Moore, K. R. Zavadil, N. M. Markovic, *ACS Catal.* **2015**, *5*, 6600–6607.
- [3] I. Ledezma-Yanez, W. D. Z. Wallace, P. Sebastián-Pascual, V. Climent, J. M. Feliu, M. T. M. Koper, *Nat. Energy* **2017**, *2*, 17031.
- [4] E. Santos, P. Quaino, W. Schmickler, *Phys. Chem. Chem. Phys.* **2012**, *14*, 11224.
- [5] A. Rendón-Calle, S. Builes, F. Calle-Vallejo, *Appl. Catal. B* **2020**, *276*, 119147.
- [6] J. Rossmeisl, K. Chan, R. Ahmed, V. Tripković, M. E. Björketun, *Phys. Chem. Chem. Phys.* **2013**, *15*, 10321.
- [7] S. Sakong, A. Groß, *Phys. Chem. Chem. Phys.* **2020**, *22*, 10431–10437.
- [8] A. Groß, F. Gossenberger, X. Lin, M. Naderian, S. Sakong, T. Roman, *J. Electrochem. Soc.* **2014**, *161*, E3015–E3020.
- [9] S. Schnur, A. Groß, *New J. Phys.* **2009**, *11*, 125003.
- [10] M. F. Toney, J. N. Howard, J. Richer, G. L. Borges, J. G. Gordon, O. R. Melroy, D. G. Wiesler, D. Yee, L. B. Sorensen, *Nature* **1994**, *368*, 444–446.
- [11] T. Iwasita, X. Xia, *J. Electroanal. Chem.* **1996**, *411*, 95–102.
- [12] S. Trasatti, *J. Electroanal. Chem. Interfacial Electrochem.* **1971**, *33*, 351–378.
- [13] R. Subbaraman, D. Tripkovic, D. Strmcnik, K.-C. Chang, M. Uchimura, A. P. Paulikas, V. Stamenkovic, N. M. Markovic, *Science* **2011**, *334*, 1256–1260.
- [14] R. Subbaraman, D. Tripkovic, K.-C. Chang, D. Strmcnik, A. P. Paulikas, P. Hirunsit, M. Chan, J. Greeley, V. Stamenkovic, N. M. Markovic, *Nat. Mater.* **2012**, *11*, 550–557.
- [15] R. Parsons, *Trans. Faraday Soc.* **1958**, *54*, 1053.
- [16] H. Gerischer, *Bull. Soc. Chim. Belg.* **2010**, *67*, 506–527.
- [17] S. Trasatti, *J. Electroanal. Chem. Interfacial Electrochem.* **1972**, *39*, 163–184.
- [18] J. K. Nørskov, T. Bligaard, A. Logadottir, J. R. Kitchin, J. G. Chen, S. Pandalov, U. Stimming, *J. Electrochem. Soc.* **2005**, *152*, J23.
- [19] M. T. M. Koper, *J. Solid State Electrochem.* **2016**, *20*, 895–899.
- [20] P. Quaino, F. Juarez, E. Santos, W. Schmickler, *Beilstein J. Nanotechnol.* **2014**, *5*, 846–854.
- [21] A. R. Zeradjanin, J.-P. Grote, G. Polymeros, K. J. J. Mayrhofer, *Electroanalysis* **2016**, *28*, 2256–2269.
- [22] A. R. Zeradjanin, A. Vimalanandan, G. Polymeros, A. A. Topalov, K. J. J. Mayrhofer, M. Rohwerder, *Phys. Chem. Chem. Phys.* **2017**, *19*, 17019–17027.
- [23] A. R. Zeradjanin, *Curr. Opin. Electrochem.* **2018**, *9*, 214–223.
- [24] A. R. Zeradjanin, G. Polymeros, C. Toparli, M. Ledendecker, N. Hodnik, A. Erbe, M. Rohwerder, F. La Mantia, *Phys. Chem. Chem. Phys.* **2020**, *22*, 8768–8780.
- [25] A. R. Zeradjanin, P. Narangoda, I. Spanos, J. Masa, R. Schlögl, *Electrochim. Acta* **2021**, *388*, 138583.
- [26] D. Strmcnik, M. Uchimura, C. Wang, R. Subbaraman, N. Danilovic, D. van der Vliet, A. P. Paulikas, V. R. Stamenkovic, N. M. Markovic, *Nat. Chem.* **2013**, *5*, 300–306.
- [27] J. O. Bockris, A. Gochev, *J. Electroanal. Chem. Interfacial Electrochem.* **1986**, *214*, 655–674.
- [28] R. Guidelli, R. G. Compton, J. M. Feliu, E. Gileadi, J. Lipkowski, W. Schmickler, S. Trasatti, *Pure Appl. Chem.* **2014**, *86*, 245–258.
- [29] B. E. Conway, D. F. Tessier, D. P. Wilkinson, *J. Electrochem. Soc.* **1989**, *136*, 2486–2493.
- [30] A. Damjanovic, A. L. Utz, A. T. Walsh, *J. Phys. Chem.* **1993**, *97*, 9177–9180.
- [31] M. Mozurkewich, S. W. Benson, *J. Phys. Chem.* **1984**, *88*, 6429–6435.
- [32] E. Sargeant, A. Kolodziej, C. S. Le Duff, P. Rodriguez, *ACS Catal.* **2020**, *10*, 7464–7474.
- [33] A. Rendón-Calle, Q. H. Low, S. H. L. Hong, S. Builes, B. S. Yeo, F. Calle-Vallejo, *Appl. Catal. B* **2021**, *285*, 119776.
- [34] A. M. Patel, S. Vijay, G. Kastlunger, J. K. Nørskov, K. Chan, *J. Phys. Chem. Lett.* **2021**, *12*, 5193–5200.
- [35] X. Nie, M. R. Esopi, M. J. Janik, A. Asthagiri, *Angew. Chem. Int. Ed.* **2013**, *52*, 2459–2462; *Angew. Chem.* **2013**, *125*, 2519–2522.
- [36] T. Shinagawa, A. T. Garcia-Esparza, K. Takanahe, *Sci. Rep.* **2015**, *5*, 13801.
- [37] N. Dubouis, A. Grimaud, *Chem. Sci.* **2019**, *10*, 9165–9181.
- [38] F. Calle-Vallejo, N. G. Inoglu, H.-Y. Su, J. I. Martínez, I. C. Man, M. T. M. Koper, J. R. Kitchin, J. Rossmeisl, *Chem. Sci.* **2013**, *4*, 1245.
- [39] Z. He, Y. Chen, E. Santos, W. Schmickler, *Angew. Chem. Int. Ed.* **2018**, *57*, 7948–7956; *Angew. Chem.* **2018**, *130*, 8076–8085.
- [40] Z.-D. He, J. Wei, Y.-X. Chen, E. Santos, W. Schmickler, *Electrochim. Acta* **2017**, *255*, 391–395.
- [41] A. R. Zeradjanin, I. Spanos, J. Masa, M. Rohwerder, R. Schlögl, *J. Solid State Electrochem.* **2021**, *25*, 33–42, DOI 10.1007/s10008-020-04815-8.
- [42] V. R. Stamenkovic, B. Fowler, B. S. Mun, G. Wang, P. N. Ross, C. A. Lucas, N. M. Markovic, *Science* **2007**, *315*, 493–497.
- [43] R. R. Dogonadze, L. I. Krishtalik, *Russ. Chem. Rev.* **1975**, *44*, 938–945.
- [44] J. O. Bockris, D. B. Matthews, *J. Chem. Phys.* **1966**, *44*, 298–309.
- [45] B. E. Conway, *Can. J. Chem.* **1959**, *37*, 178–189.
- [46] J. Durst, A. Siebel, C. Simon, F. Hasché, J. Herranz, H. A. Gasteiger, *Energy Environ. Sci.* **2014**, *7*, 2255–2260.
- [47] J. Durst, C. Simon, F. Hasché, H. A. Gasteiger, *J. Electrochem. Soc.* **2015**, *162*, F190–F203.
- [48] A. R. Zeradjanin, *ChemSusChem* **2018**, *11*, 1278–1284.
- [49] A. R. Zeradjanin, P. Narangoda, I. Spanos, J. Masa, R. Schlögl, *Curr. Opin. Electrochem.* **2021**, *30*, 100797.
- [50] H. A. El-Sayed, A. Weiß, L. F. Olbrich, G. P. Putro, H. A. Gasteiger, *J. Electrochem. Soc.* **2019**, *166*, F458–F464.
- [51] D. Strmcnik, K. Kodama, D. van der Vliet, J. Greeley, V. R. Stamenkovic, N. M. Marković, *Nat. Chem.* **2009**, *1*, 466–472.
- [52] D. Y. Chung, P. P. Lopes, P. F. B. D. Martins, H. He, T. Kawaguchi, P. Zapol, H. You, D. Tripkovic, D. Strmcnik, Y. Zhu, S. Seifert, S. Lee, V. R. Stamenkovic, N. M. Markovic, *Nat. Energy* **2020**, *5*, 222–230.

- [53] I. Spanos, J. Masa, A. Zeradjanin, R. Schlögl, *Catal. Lett.* **2021**, *151*, 1843–1856.
- [54] S. Trasatti, *Russ. J. Electrochem.* **2005**, *41*, 1255–1264.
- [55] O. Pecina, W. Schmickler, *Chem. Phys.* **1998**, *228*, 265–277.
- [56] D. Teschner, G. Novell-Leruth, R. Farra, A. Knop-Gericke, R. Schlögl, L. Szentmiklósi, M. G. Hevia, H. Soerijanto, R. Schomäcker, J. Pérez-Ramírez, N. López, *Nat. Chem.* **2012**, *4*, 739–745.
- [57] T. Bligaard, K. Honkala, A. Logadottir, J. K. Nørskov, S. Dahl, C. J. H. Jacobsen, *J. Phys. Chem. B* **2003**, *107*, 9325–9331.
- [58] G. C. Bond, M. A. Keane, H. Kral, J. A. Lercher, *Catal. Rev.* **2000**, *42*, 323–383.
- [59] E. Cremer, in *Adv. Catal.*, Elsevier, **1955**, pp. 75–91.
- [60] A. K. Galwey, in *Adv. Catal.*, Elsevier, **1977**, pp. 247–322.
- [61] D. Koster, A. R. Zeradjanin, A. Battistel, F. La Mantia, *Electrochim. Acta* **2019**, *308*, 328–336.

Manuscript received: September 18, 2021

Revised manuscript received: November 2, 2021

Accepted manuscript online: November 2, 2021